Supporting Information

A paradigm study of polymer donor diluted bulk heterojunction film for application in semitransparent organic photovoltaics

Zhenyu Chen,[a] Wei Ma[a] and Han Yan*[a]

State Key Laboratory for Mechanical Behavior of Materials, School of Materials Science and Engineering, Xi'an Jiaotong University, Xi'an 710049, China. E-mail: mseyanhan@xjtu.edu.cn

Experimental section

Materials: PM6 and D18 were purchased from Solarmer Materials Inc. Y6 was purchased from eFlexPV Inc. N-DMBI, chloroform (CF) and methanol were purchased from Sigma-Aldrich. 1-chloronaphthalene (CN) was purchased from TCI. All chemicals were used as received without further purification.

Instrumentation: The GIWAXS measurements of the control and doped films were performed at beamline 7.3.3[1] at the Advanced Light Source. Samples were prepared on Si substrates using identical blend solutions as those used in devices. The 10 keV X-ray beam was incident at a grazing angle of 0.11°-0.15°. The scattered x-ray was detected using a Dectris Pilatus 2M photon counting detector. The *J*–*V* curves were performed in the N2-filled glovebox under AM 1.5G (100 mW cm^{-2}) using an AAA solar simulator (SS-F5-3A, Enli Technology Co., Ltd.) calibrated with astandard photovoltaic cell equipped with KG5 filter. The EQE curves were measured by Solar Cell Spectral Response Measurement System QE-R3018 (Enli Technology Co., Ltd.) with calibrated light intensity by a standard Si photovoltaic cell. The absorbance and transmittance were obtained on a Shimadzu UV-3600. PL spectrum was recorded by FLS980 spectrometer (Edinburgh Instruments, EI) with different excitation wavelength. AFM images were obtained by Bruker INNOVA.

Device fabrications: Organic solar cells were fabricated on ITO glass substrates with the conventional structure of ITO/PEDOT: PSS/Active layer/PDINO/Ag (or ultra-thin Ag for ST-OSCs). The patterned ITO substrates were sequentially cleaned by deionized water, acetone, and isopropanol for 30 min in each step before fabrication. The pre-cleaned ITO substrates were treated in an ultraviolet ozone generator for 15 min, followed by spin-coating the PEDOT:PSS layer

at 5000 rpm for 30 s. After baking the PEDOT:PSS layer in air at 150 °C for 15 min, the substrates were transferred to a glovebox. The spin-coating condition of active layer was listed in the Table below. For the N-DMBI doping devices, suitable content of dopant solutions (use CF as the solvent) were added into the blend solution for 30 min stirring before coating. For the PM6:Y6 devices, the blend films were annealed at 100 °C for 10 min. A layer of PDINO (0.5 mg mL-1 in methanol) was deposited by spin-coating at 5000 rpm for 20 s. Then the Ag electrode with varied thickness was deposited by thermal evaporation under a base pressure of 1×10^{-5} Pa. To further improve the ST-OSCs, a MoO_3 layer (35 nm) was deposited on the ultra-thin Ag electrode under a pressure of 1×10^{-5} Pa.

Table of spin-coating conditions for devices mentioned in this paper

Samples	D/A ratio	Concentration	spin coating condition
PM6:Y6	1:1.2 (BHJ)	16 mg/mL	4000 rpm
	0.40:1	18 mg/mL	6000 rpm
	0.35:1	17 mg/mL	5000 rpm
	0.30:1	17 mg/mL	5000 rpm
	0.25:1	16 mg/mL	4500 rpm
	0.20:1	16 mg/mL	3500 rpm
D18:Y6	1:1.6 (BHJ)	11 mg/mL	3000 rpm
	0.40:1	13 mg/mL	2500 rpm
	0.35:1	12 mg/mL	4000 rpm
	0.30:1	12 mg/mL	3000 rpm
	0.25:1	11 mg/mL	4000 rpm
	0.20:1	11 mg/mL	3000 rpm

Calculation of the average visible transmittance (AVT)： The AVT value was calculated according to the average value of transmittance of semitransparent devices based on photonic response of the human eye. The wavelength range is usually adopted by 380-760nm, and the specific calculation formula is

$$AVT = \frac{\int T(\lambda)F(\lambda)E(\lambda)d\lambda}{\int F(\lambda)E(\lambda)d\lambda} \quad \text{S1}$$

where T(λ) is the transmission spectra of semi-transparent devices, F(λ) is photon flux under AM 1.5G light illumination conditions, and E(λ) is the photonic response of the human eye.

SCLC Measurements：The charge carrier mobilities of the blend films were measured using the space-charge-limited current (SCLC) method. Electron-only devices were fabricated in the structure of ITO/ZnO/active layer/PDINO/Ag, and hole-only devices were fabricated in the structure of ITO/PEDOT: PSS/active layer/MoO_3/Ag. The device characteristics were extracted by modeling the dark current under forwarding bias using the SCLC expression described by the Mott-Gurney law described by equation S2:

$$J = \frac{9}{8}\varepsilon_r\varepsilon_0\mu\frac{V^2}{L^3} \quad \text{S2}$$

where ε_r = 3 is the average dielectric constant of organic materials, ε_0 is the vacuum dielectric constant, μ is the carrier mobility, L is the thickness of the film, and V is the applied voltage.

Calculation of the color coordinates: The color coordinates (x, y, z) of semitransparent devices were calculated according to the transmission spectra based on chromaticity diagram of the CIE 1931xy. The color coordinates were calculated by the formulas:

$$\begin{cases} X = \int \varphi(\lambda) \times \bar{x}(\lambda) \times d\lambda \\ Y = \int \varphi(\lambda) \times \bar{y}(\lambda) \times d\lambda \\ Z = \int \varphi(\lambda) \times \bar{z}(\lambda) \times d\lambda \end{cases} \quad \text{S3}$$

$$\begin{cases} x = \dfrac{X}{X+Y+Z} \\ x = \dfrac{Y}{X+Y+Z} \\ x = \dfrac{Z}{X+Y+Z} \end{cases} \quad \text{S4}$$

where X, Y, Z are tristimulus values, φ(λ) is the spectral power distribution (SPD) of the transmission spectra of semi-transparent devices and $\bar{x}(\lambda)$, $\bar{y}(\lambda)$, $\bar{z}(\lambda)$ are color-matching functions. The sum of x,y,z coordinates is equal to 1. Therefore, the 3D color coordinates (x,y,z) can be simplified into 2D color coordinates (x,y). The color coordinates (x, y) of a solar cell can be calculated by the product of the transmission spectrum of the device and the incident light

spectrum.

Calculation of the CRI and CCT: The CRI quantitatively expresses the degree of color appearances to the real objects with values of CRI ranging from 0 to 100. It was calculated by the CIE 1931xy chromaticity diagram. We obtained all the CRI and CCT values by using the software "color tool".

Supporting Figures:

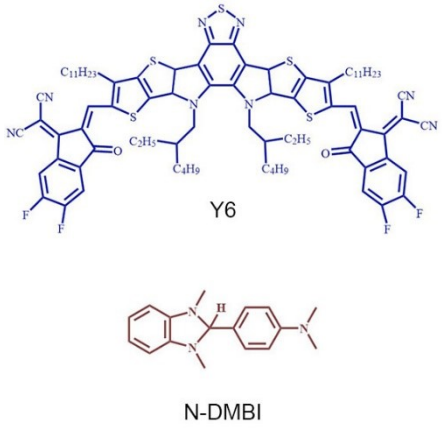

Fig. S1 Chemical structures of Y6 and N-DMBI.

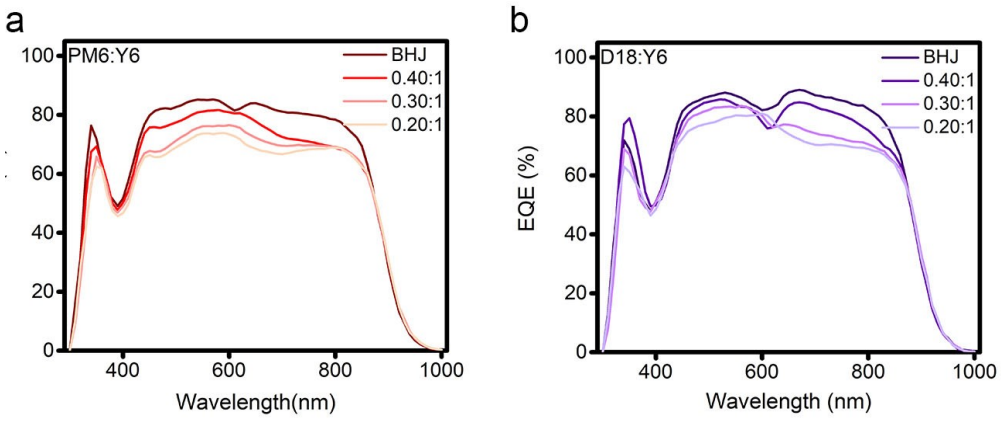

Fig. S2 EQE curves of PM6 diluted PM6:Y6 devices (a) and D18 diluted D18:Y6 devices (b).

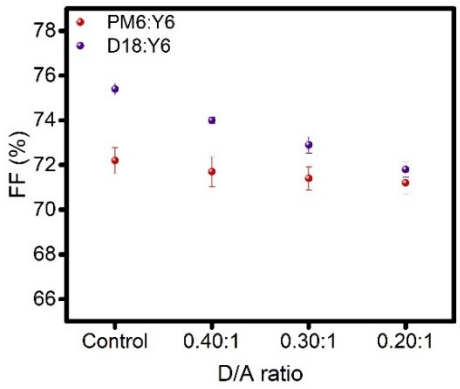

Fig. S3 Comparison of FF for PM6:Y6 and D18:Y6 diluted opaque devices with different D/A ratio.

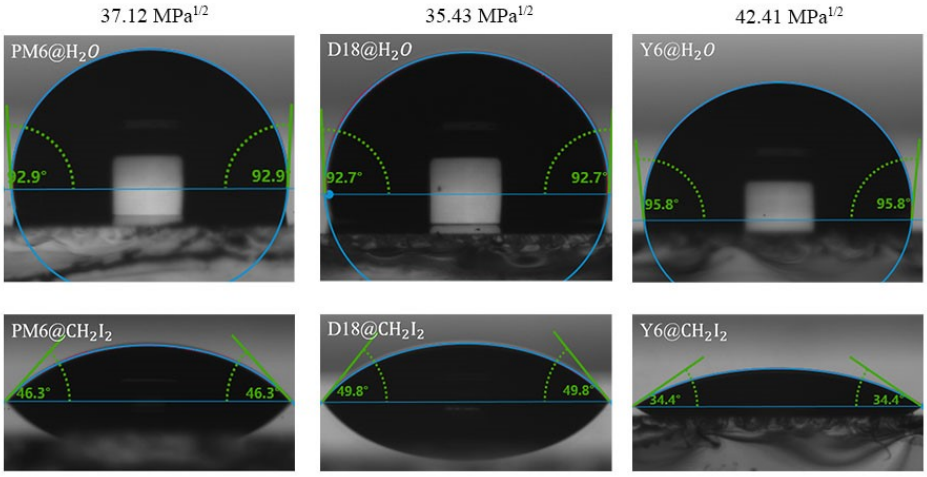

Fig. S4 Contact angles of PM6, D18, and Y6 neat films.

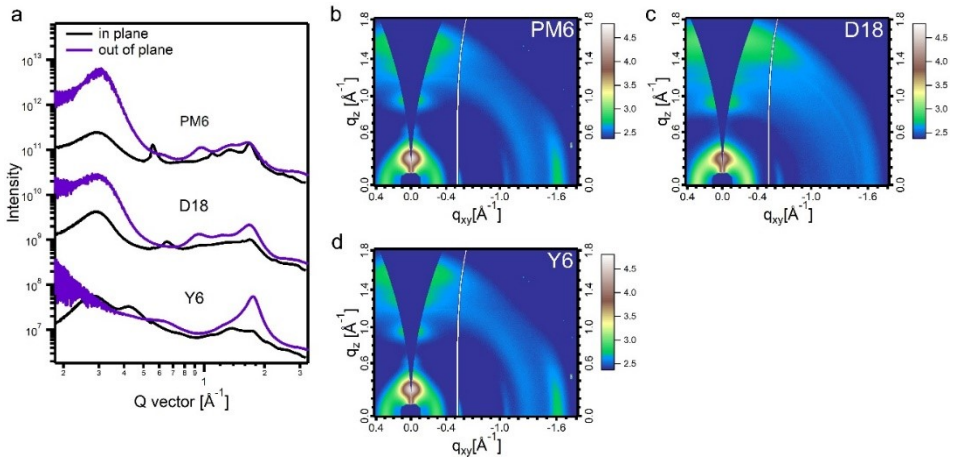

Fig. S5 (a) In plane and out of plane line cuts of the GIWAXS patterns for PM6, D18, and Y6 neat films. (b, c, d) Corresponding two-dimensional GIWAXS patterns of (b) PM6; (c) D18, and (d) Y6 neat films.

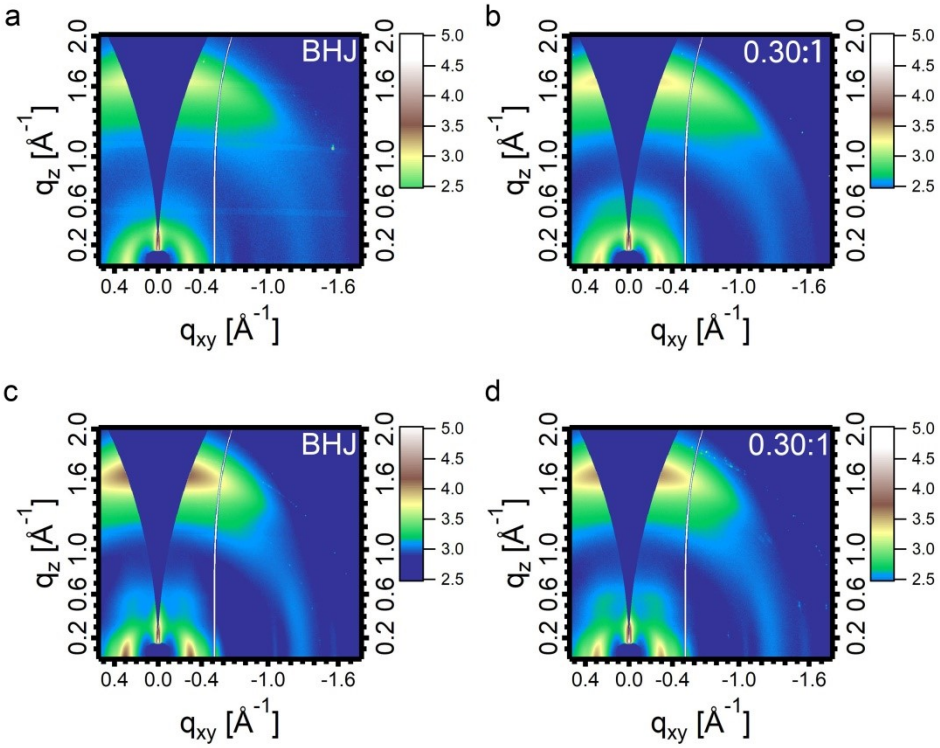

Fig. S6 (a, b) 2D patterns of GIWAXS for (a) BHJ and (b) 0.30:1 donor diluted PM6:Y6 films. (c, d) 2D patterns of GIWAXS for (c) BHJ and (d) 0.30:1 donor diluted D18:Y6 films.

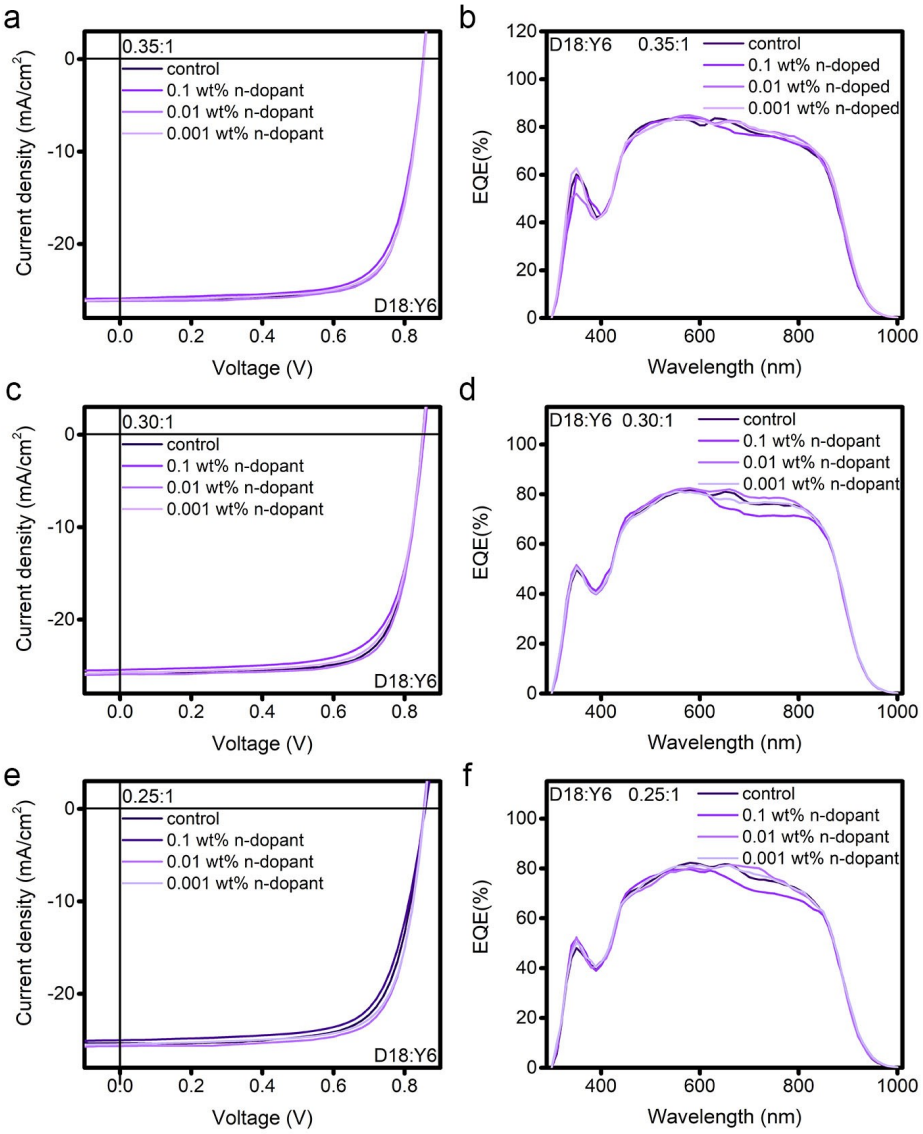

Fig. S7 Photovoltaic performances of D18 diluted (0.35:1, 0.30:1, 0.25:1) D18:Y6 devices. (a, c, e) J-V curves of (a) 0.35:1, (c) 0.30:1, and (e) 0.25:1 donor diluted devices. (b, d, f) Corresponding EQE spectra of (b) 0.35:1, (d) 0.30:1, and (f) 0.25:1 donor diluted devices.

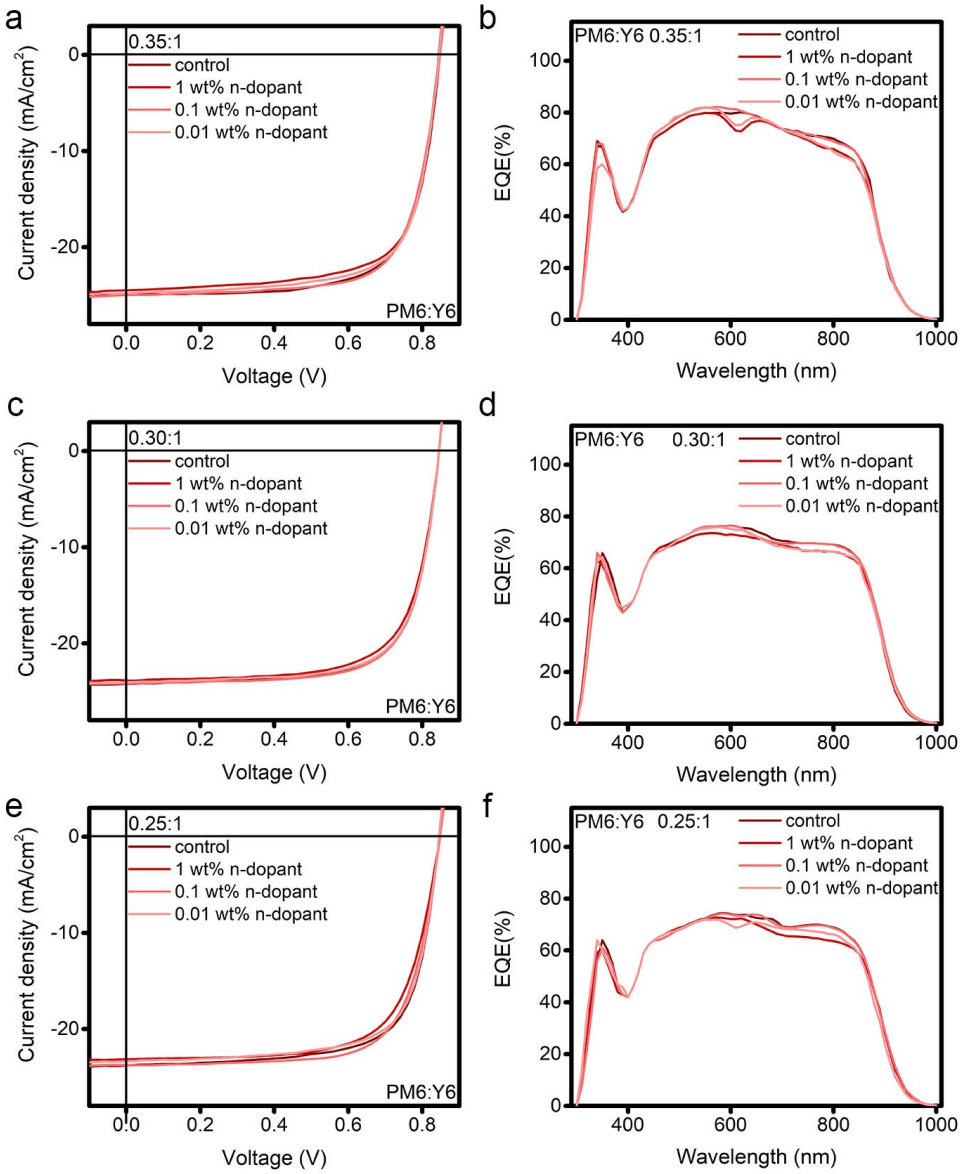

Fig. S8 Photovoltaic performances of PM6 diluted (0.35:1, 0.30:1, 0.25:1) PM6:Y6 devices. (a, c, e) J-V curves of (a) 0.35:1, (c) 0.30:1, and (e) 0.25:1 donor diluted devices. (b, d, f) Corresponding EQE spectra of (b) 0.35:1, (d) 0.30:1 and (f) 0.25:1 donor diluted devices.

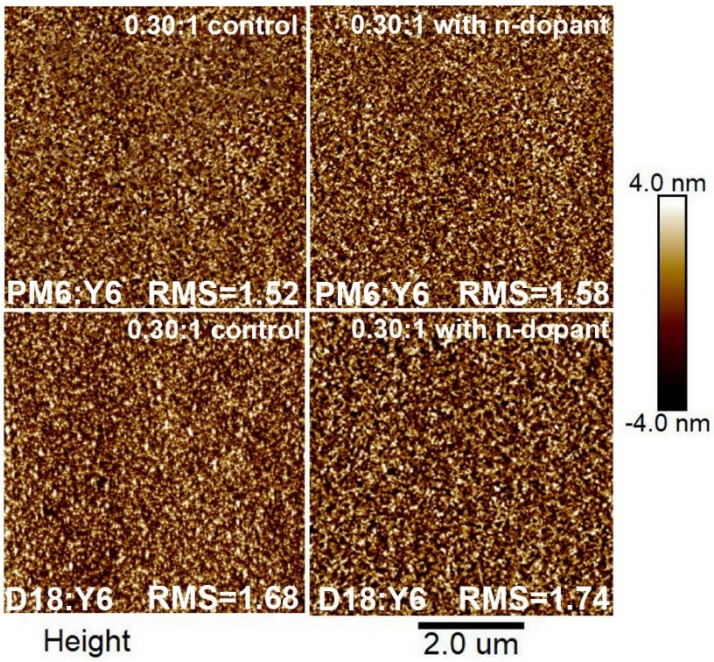

Fig. S9 AFM images of PM6:Y6 and D18:Y6 with and without N-DMBI.

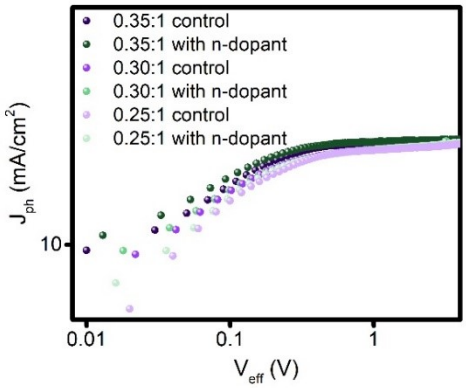

Fig. S10 J_{ph} curves of D18 diluted (0.35:1, 0.30:1, 0.25:1) D18:Y6 devices with or without N-DMBI.

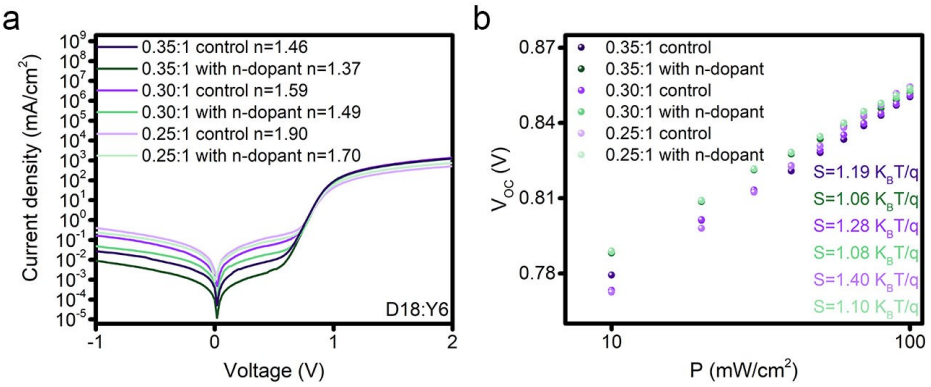

Fig. S11 (a) Dark current of D18 diluted (0.35:1, 0.30:1, 0.25:1) D18:Y6 devices with or without N-DMBI. (b) V_{OC} versus light intensity plots of D18 diluted D18:Y6 opaque devices.

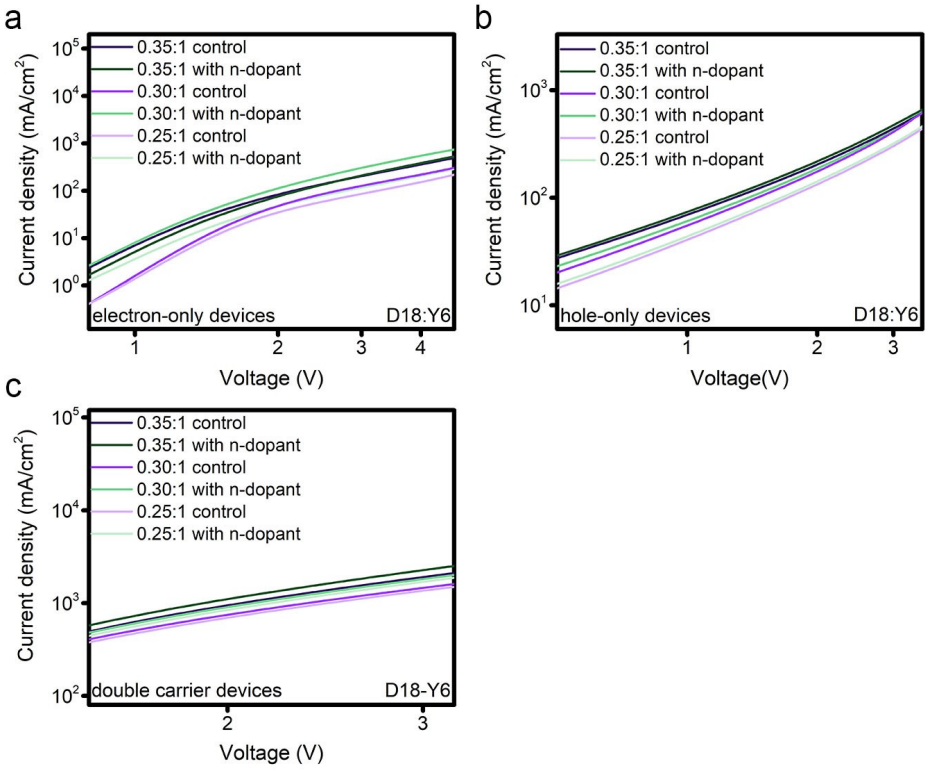

Fig. S12 *J*–*V* curves of D18:Y6-based (a) electron-only devices, (b) hole-only devices, and (c) double carrier devices.

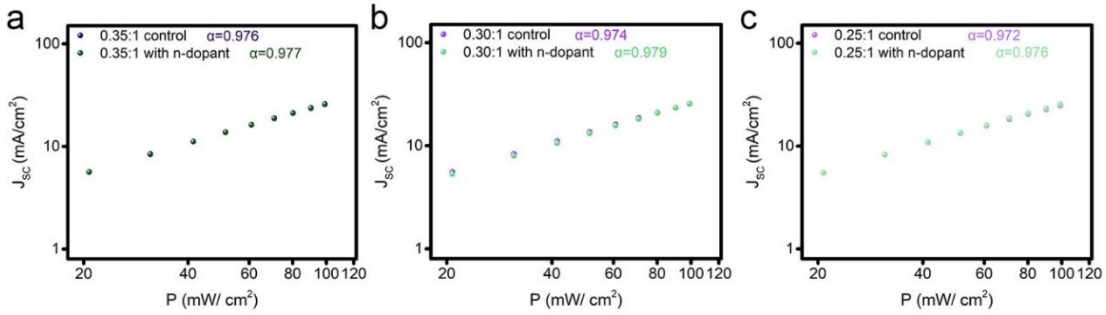

Fig. S13 The J_{SC} versus light intensity plots of D18 diluted D18:Y6 opaque devices.

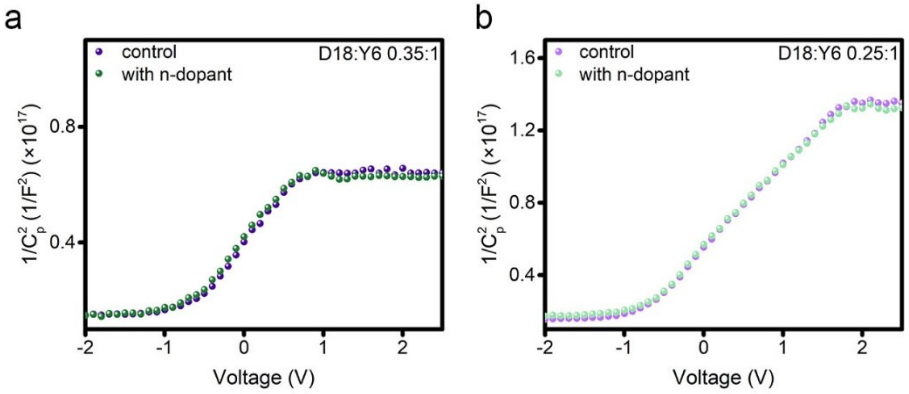

Fig. S14. Capacitance versus DC bias of (a) 0.35:1 and (b) 0.25:1 D18 diluted D18:Y6 MIS samples.

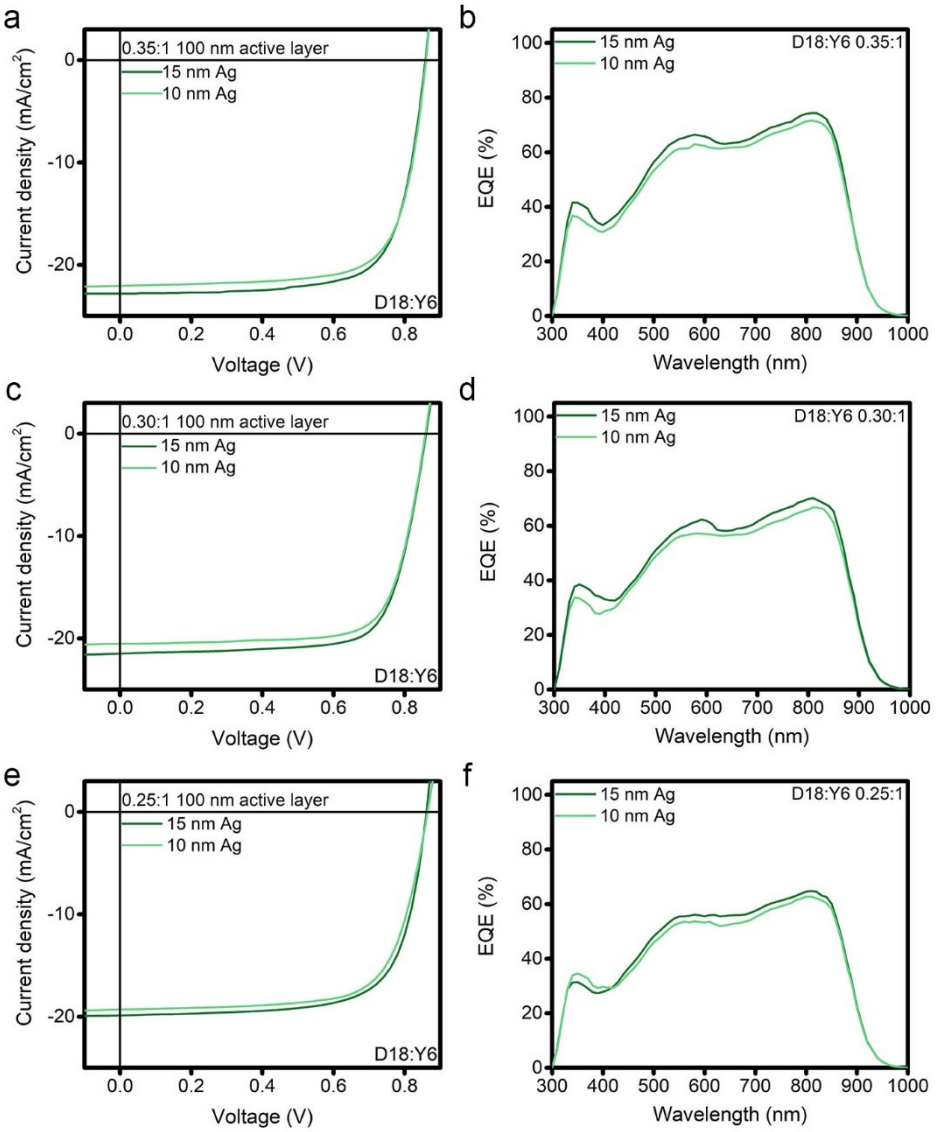

Fig. S15 *J-V* curves and corresponding EQE spectra of D18 diluted D18:Y6 ST-OSCs with different thickness of Ag electrode. (a, c, e) *J-V* curves of 0.35:1, 0.30:1, and 0.25:1 donor diluted ST-OSCs. (b, d, f) The corresponding EQE spectra of *J-V* curves.

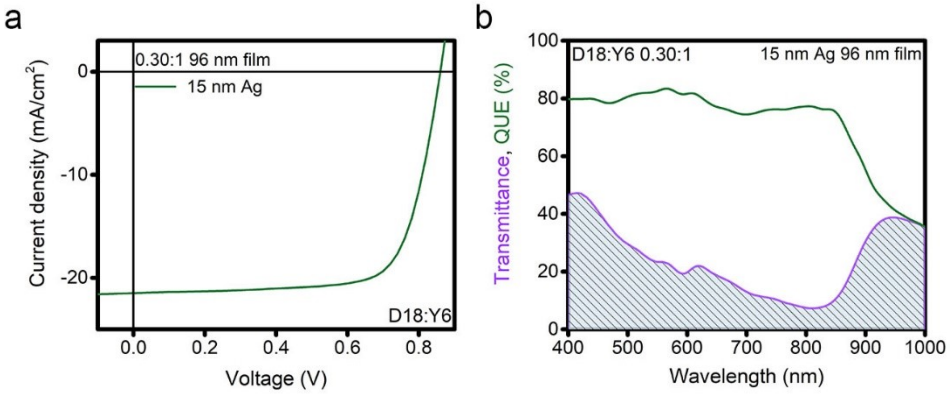

Fig. S16 (a) *J-V* curves and (b) corresponding transmittance spectra as well as QUE curve of D18 diluted D18:Y6 ST-OSCs with 96 nm film and 15 nm Ag electrode.

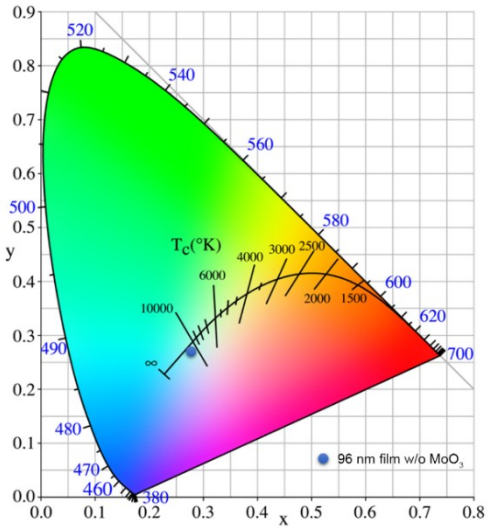

Fig. S17 Color coordinates of ST-OSC with 96 nm film and 15 nm Ag electrode on a CIE 1931xy chromaticity diagram.

Supporting Tables:

Table S1 AVT values of PM6 diluted PM6:Y6 films.

Conditions	AVT（blend film）
BHJ	36.57%
0.40:1	45.36%
0.30:1	51.93%
0.20:1	54.21%

Table S2 AVT values of D18 diluted D18:Y6 films

Conditions	AVT（blend film）
BHJ	42.05%
0.40:1	51.81%
0.30:1	59.82%
0.20:1	62.01%

Table S3 Photovoltaic properties of PM6 diluted PM6:Y6 opaque devices.

Conditions	V_{OC} (V)	J_{SC} (mA/cm^2)	J_{SC} (EQE) (mA/cm^2)	FF (%)	PCE (Ave. ±Dev.)[a] (%)
PM6:Y6 BHJ (1:1.2)	0.843	27.23	26.37	72.8	16.70 (16.55±0.16)
PM6:Y6 0.40:1	0.844	25.29	24.36	72.3	15.43 (15.25±0.18)
PM6:Y6 0.30:1	0.845	24.31	23.23	71.5	14.67 (14.41±0.21)
PM6:Y6 0.20:1	0.846	23.59	22.85	70.9	14.15 (14.03±0.12)

[a] Averaged values in parentheses are from 10 devices.

Table S4 Photovoltaic properties of D18 diluted D18:Y6 opaque devices.

Conditions	V_{OC} (V)	J_{SC} (mA/cm^2)	J_{SC} (EQE) (mA/cm^2)	FF (%)	PCE (Ave. ±Dev.)[a] (%)
D18:Y6 BHJ (1:1.6)	0.852	27.85	27.09	75.9	18.01 (17.93±0.06)
D18:Y6 0.40:1	0.852	26.50	25.51	74.2	16.75 (16.67±0.06)
D18:Y6 0.30:1	0.851	25.74	24.65	72.9	15.97 (15.82±0.11)
D18:Y6 0.20:1	0.854	24.84	24.10	71.8	15.23 (15.12±0.08)

[a] Averaged values in parentheses are from 10 devices.

Table S5 D-spacing and CL values for PM6:Y6 GIWAXS data.

OOP π-π	Conditions	q ($Å^{-1}$)	d-spacing (Å)	CL (Å)
	BHJ	1.73	3.63	24.91
	0.30:1	1.74	3.61	26.55
IP lamellar	**Conditions**	**q ($Å^{-1}$)**	**d-spacing (Å)**	**CL (Å)**
	BHJ	0.29	21.67	65.75
	0.30:1	0.29	21.67	67.32
IP Y6(11-1)	**Conditions**	**q ($Å^{-1}$)**	**d-spacing (Å)**	**CL (Å)**
	BHJ	0.38	17.45	30.57
	0.30:1	0.39	16.11	39.82

Table S6 D-spacing and CL values for D18:Y6 GIWAXS data.

OOP π-π	Conditions	q ($Å^{-1}$)	d-spacing (Å)	CL (Å)
	BHJ	1.72	3.65	27.82
	0.30:1	1.73	3.63	28.12
IP lamellar	**Conditions**	**q ($Å^{-1}$)**	**d-spacing (Å)**	**CL (Å)**
	BHJ	0.31	20.27	83.23
	0.30:1	0.30	20.94	77.52
IP Y6(11-1)	**Conditions**	**q ($Å^{-1}$)**	**d-spacing (Å)**	**CL (Å)**
	BHJ	0.38	16.53	43.52
	0.30:1	0.39	16.11	46.71
IP D18 (002)	**Conditions**	**q ($Å^{-1}$)**	**d-spacing (Å)**	**CL (Å)**
	BHJ	0.55	11.42	188.51
	0.30:1	0.55	11.42	144.54

Table S7 Photovoltaic properties of D18 diluted D18:Y6 opaque devices (0.35:1) with and without N-DMBI.

Conditions	V_{OC} (V)	J_{SC} (mA/cm^2)	J_{SC} (EQE) (mA/cm^2)	FF (%)	PCE (Ave. ±Dev.)[a] (%)
control	0.850	26.05	25.05	74.4	16.55 (16.36±0.17)
0.1 wt% N-DMBI	0.853	25.88	24.90	73.1	16.14 (15.96±0.16)
0.01 wt% N-DMBI	0.852	26.16	25.30	75.6	16.86 (16.85±0.14)
0.001 wt% N-DMBI	0.850	26.02	25.15	74.3	16.43 (16.28±0.14)

[a] Averaged values in parentheses are from 10 devices.

Table S8 Photovoltaic properties of D18 diluted D18:Y6 opaque devices (0.30:1) with and without N-DMBI.

Conditions	V_{OC} (V)	J_{SC} (mA/cm^2)	J_{SC} (EQE) (mA/cm^2)	FF (%)	PCE (Ave. ±Dev.)[a] (%)
control	0.851	25.74	24.70	72.9	15.97 (15.82±0.11)
0.1 wt% N-DMBI	0.854	25.43	24.18	71.8	15.59 (15.50±0.09)
0.01 wt% N-DMBI	0.853	25.89	24.95	75.7	16.71 (16.58±0.18)
0.001 wt% N-DMBI	0.851	25.70	24.60	73.7	16.12 (15.95±0.15)

[a] Averaged values in parentheses are from 10 devices.

Table S9 Photovoltaic properties of D18 diluted D18:Y6 opaque devices (0.25:1) with and without N-DMBI.

Conditions	V_{OC} (V)	J_{SC} (mA/cm^2)	J_{SC} (EQE) (mA/cm^2)	FF (%)	PCE (Ave. ±Dev.)[a] (%)
control	0.854	25.36	24.38	71.8	15.58 (15.49±0.09)
0.1 wt% N-DMBI	0.857	25.01	23.81	70.5	15.11 (15.02±0.09)
0.01 wt% N-DMBI	0.854	25.64	24.55	74.2	16.25 (16.20±0.06)
0.001 wt% N-DMBI	0.854	25.44	24.47	73.1	15.88 (15.77±0.11)

[a] Averaged values in parentheses are from 10 devices.

Table S10 Photovoltaic properties of PM6 diluted PM6:Y6 opaque devices (0.35:1) with and without N-DMBI.

Conditions	V_{OC} (V)	J_{SC} (mA/cm^2)	J_{SC} (EQE) (mA/cm^2)	FF (%)	PCE (Ave. ±Dev.)[a] (%)
control	0.845	24.85	23.90	71.5	15.00 (14.96±0.03)
1 wt% N-DMBI	0.848	24.42	23.43	70.5	14.60 (14.53±0.06)
0.1 wt% N-DMBI	0.848	24.98	24.08	71.3	15.10 (15.05±0.05)
0.01 wt% N-DMBI	0.847	24.78	23.70	71.2	14.94 (14.90±0.04)

[a] Averaged values in parentheses are from 10 devices.

Table S11 Photovoltaic properties of PM6 diluted PM6:Y6 opaque devices (0.30:1) with and without N-DMBI.

Conditions	V_{OC} (V)	J_{SC} (mA/cm^2)	J_{SC} (EQE) (mA/cm^2)	FF (%)	PCE (Ave. ±Dev.)[a] (%)
control	0.845	24.31	23.23	71.5	14.67 (14.41±0.21)
1 wt% N-DMBI	0.847	23.85	22.75	70.2	14.18 (14.10±0.08)
0.1 wt% N-DMBI	0.845	24.17	23.06	71.7	14.64 (14.56±0.06)
0.01 wt% N-DMBI	0.846	24.05	22.96	71.1	14.47 (14.34±0.11)

[a] Averaged values in parentheses are from 10 devices.

Table S12 Photovoltaic properties of PM6 diluted PM6:Y6 opaque devices (0.25:1) with and without N-DMBI.

Conditions	V_{OC} (V)	J_{SC} (mA/cm^2)	J_{SC} (EQE) (mA/cm^2)	FF (%)	PCE (Ave. ±Dev.)[a] (%)
control	0.845	23.78	22.60	70.9	14.26 (14.13±0.13)
1 wt% N-DMBI	0.847	23.15	22.05	69.3	13.59 (13.50±0.09)
0.1 wt% N-DMBI	0.846	23.74	22.54	71.0	14.26 (14.18±0.08)
0.01 wt% N-DMBI	0.846	23.35	22.25	70.5	13.93 (13.85±0.08)

[a] Averaged values in parentheses are from 10 devices.

Table S13 Hole mobility, electron mobility, double carrier mobility of D18 diluted D18:Y6 devices by SCLC measurement and Langevin prefactor (γ_{pre}) calculated by the mobility data.

Conditions	Hole mobility ($cm^2V^{-1}s^{-1}$)	Electron mobility ($cm^2V^{-1}s^{-1}$)	H/E ratio	Double carrier mobility ($cm^2V^{-1}s^{-1}$)	γ_{pre} (10^{-2})
0.35:1 control	$1.20\times10^{-4}\pm1.1\times10^{-5}$	$5.86\times10^{-5}\pm5.39\times10^{-6}$	2.04	$7.64\times10^{-4}\pm1.25\times10^{-5}$	8.4
0.35:1 with 0.01 wt% N-DMBI	$1.24\times10^{-4}\pm1.1\times10^{-5}$	$7.95\times10^{-5}\pm5.39\times10^{-6}$	1.56	$9.20\times10^{-4}\pm1.20\times10^{-5}$	6.8
0.30:1 control	$1.06\times10^{-4}\pm3.0\times10^{-6}$	$3.58\times10^{-5}\pm4.26\times10^{-6}$	2.96	$5.59\times10^{-4}\pm6.94\times10^{-6}$	7.2
0.30:1 with 0.01 wt% N-DMBI	$1.08\times10^{-4}\pm3.0\times10^{-6}$	$5.11\times10^{-5}\pm5.47\times10^{-6}$	2.11	$7.08\times10^{-4}\pm1.19\times10^{-5}$	6.4
0.25:1 control	$9.34\times10^{-5}\pm1.2\times10^{-6}$	$2.09\times10^{-5}\pm3.46\times10^{-6}$	4.47	$4.90\times10^{-4}\pm8.26\times10^{-6}$	4.4
0.25:1 with 0.01 wt% N-DMBI	$9.51\times10^{-5}\pm4.6\times10^{-6}$	$3.39\times10^{-5}\pm4.71\times10^{-6}$	2.81	$6.67\times10^{-4}\pm1.76\times10^{-5}$	4.2

Table S14 Carrier density of D18 diluted D18:Y6 systems with and without N-DMBI.

	n
0.35:1 control	8.23×10^{16}
0.35:1 with 0.01 wt% N-DMBI	8.33×10^{16}
0.30:1 control	7.39×10^{16}
0.30:1 with 0.01 wt% N-DMBI	7.42×10^{16}
0.25:1 control	6.39×10^{16}
0.25:1 with 0.01 wt% N-DMBI	6.54×10^{16}

Table S15 Photovoltaic properties of D18 diluted D18:Y6 (0.35:1) semitransparent devices with different electrode thickness.

Devices (0.35:1)	V_{oc} (V)	J_{sc} (mA/cm²)	J_{sc} (EQE) (mA/cm²)	FF (%)	PCE (Ave. ±Dev.)[a] (%)	AVT (%)	LUE	Active Layer Thickness(nm)	Electrode
0.01 wt% N-DMBI	0.860	22.05	20.99	72.7	13.79 (13.72±0.05)	23.83	3.29	100	10 nm Ag
0.01 wt% N-DMBI	0.858	22.80	21.82	72.8	14.26 (14.19±0.05)	21.10	3.01	100	15m Ag

[a] Averaged values in parentheses are from 10 devices.

Table S16 Photovoltaic properties of D18 diluted D18:Y6 (0.30:1) semitransparent devices with different electrode thickness.

Devices (0.30:1)	V_{oc} (V)	J_{sc} (mA/cm²)	J_{sc} (EQE) (mA/cm²)	FF (%)	PCE (Ave. ±Dev.)[a] (%)	AVT (%)	LUE	Thickness of active layer (nm)	Electrode
0.01 wt% N-DMBI	0.858	20.53	19.52	73.9	13.02 (12.95±0.09)	26.37	3.43	96	10 nm Ag
0.01 wt% N-DMBI	0.860	21.48	20.45	73.5	13.59 (13.47±0.10)	23.72	3.22	96	15 nm Ag

[a] Averaged values in parentheses are from 10 devices.

Table S17 Photovoltaic properties of D18 diluted D18:Y6 (0.25:1) semitransparent devices with different electrode thickness.

Devices (0.25:1)	V_{oc} (V)	J_{sc} (mA/cm²)	J_{sc} (EQE) (mA/cm²)	FF (%)	PCE (Ave. ±Dev.)[a] (%)	AVT (%)	LUE	Thickness of active layer (nm)	Electrode
0.01 wt% N-DMBI	0.864	19.30	18.35	70.8	11.82 (11.72±0.07)	28.46	3.36	92	10 nm Ag
0.01 wt% N-DMBI	0.861	19.94	18.97	71.3	12.24 (12.21±0.03)	26.25	3.26	92	15 nm Ag

[a] Averaged values in parentheses are from 10 devices.

Table S18 Detailed parameter on state-of-the-art binary ST-OSC devices without optical engineering optimization reported in the literature.

Device structure	PCE (%)	AVT (%)	LUE (%)	Reference
ITO/ PEDOT:PSS)/ PM6:Y6-BO/ (PNDIT-F3N)/ Ag	11.3	30.0	3.39	2
ITO/ PEDOT:PSS/ PCE10-BDT2F-0.8:Y6/ PDINO/ Ag	11.54	26.16	3.02	3
ITO/ PEDOT:PSS/ D18:N3/ PDIN/ Au/ Ag	12.91	22.49	2.90	4
ITO/ ZnO/ PBT1-C-2Cl:Y6/ MoO_3/ Au	9.1	40.1	3.65	5
ITO/ AuNBPs-PEDOT:PSS/ PM6:BTP-eC9/ /BCP/ Au/ Ag	12.61	24.5	3.09	6
ITO/ ZnO/ PTB7-Th:IHIC/ MoO_3/ Au/ Ag	9.77	36.0	3.52	7
ITO/ ZnO/ PTB7-Th: FOIC/ MoO_3/ Au/ Ag	10.3	37.4	3.85	8
ITO/ ZnO/ PCPDTFBT:PC71BM/PEDOT:PSS/ Ag	5.0	47	2.35	9

ITO/ PEDOT:PSS/ PBDTT-FDPP-C12:PC61BM/ TiO_2/ Ag	4.0	61	2.44	10
ITO/ ZnO/PCE10-2Cl:IT-4F MoO_3/ Ag (15 nm)	9.00	25	2.25	11
ITO/ ZnO/PCE10-2Cl:IT-4F MoO_3/ Ag (10 nm)	8.25	33	2.72	11
ITO/ ZnO/ PCE-10: BT-CIC/ MoO_3/ Ag(10 nm)	7.1	43	3.05	12
ITO/ ZnO/ PCE-10: BT-CIC/ MoO_3/ Ag(20 nm)	8.2	26	2.13	12
ITO/ ZnO/ PTB7-Th:IUIC/ MoO_3/ Ag	9.9	31	3.07	13
ITO/ ZnO/ PTB7-Th:ITIC4/ MoO_3/ Ag	6.3	28	1.76	13
ITO/PEDOT:PSS/J52:IEICO-4Cl/PFN-Br/Au	6.4	35	2.24	14
ITO/PEDOT:PSS/PBDB-T:IEICO-4Cl/PFN-Br/Au	6.2	36	2.23	14
ITO/PEDOT:PSS/PTB7-Th-IEICO-4Cl/PFN-Br/Au	7.0	34	2.38	14
ITO/PEDOT:PSS/PTB7-Th:ATT-2/ MoO_3/Ag(10 nm)	6.3	45	2.84	15
ITO/PEDOT:PSS/PTB7-Th:ATT-2/ MoO_3/Ag(20 nm)	7.7	37	2.85	15
ITO/SnO2/PBDB-T:Y14/ MoO_3/Ag	12.7	24	3.05	16
ITO/ PEDOT:PSS/ PTB7-Th:PC71BM/ ZrAcac/ Ag(15 nm)	8.0	21	1.68	17
ITO/ PEDOT:PSS/ PTB7-Th:PC71BM/ ZrAcac/ Ag(5 nm)	3.8	46	1.75	17
ITO/ZnO/ PTB7-Th: F8IC/ MoO_3/ Au/ Ag	9.6	35	3.36	18
ITO/ZnO/ PTB7-Th: FOIC/ MoO_3/ Au/ Ag	9.9	31	3.07	18
ITO/ZnO/ PTB7-Th: IEICO-4F/ MoO_3/ Au/ Ag	10.0	33	3.30	18
ITO/ PEDOT:PSS/ PTB7-TF:Y6/ ZnO/ Au/ Ag	10.8	17	1.84	19
ITO/ PEDOT:PSS/ PTB7-TF:Y6 (bilayer) / ZnO/ Au/ Ag	12.2	22	2.68	19
ITO/PEDOT:PSS/PM6:Y6/PDINO/Ag NWs	9.7	42.82	4.15	20

Table S19 CIE1931 color coordinates, CCT and CRI parameters of optimized ST-OSCs with or without MoO_3.

Conditions	Ag thickness (nm)	Film thickness (nm)	MoO_3	LUE (%)	CIE1931(x,y)	CCT (K)	CRI
0.30:1	15	96	w/o	3.22	(0.278, 0.269)	11485	89.15
	10	96	w/o	3.43	(0.284, 0.278)	10137	90.56
	10	70	w/o	3.83	(0.286, 0.280)	9748	90.93
	10	70	w	4.37	(0.286, 0.287)	9326	92.49

Reference

1 A. Hexemer, W. Bras, J. Glossinger, E. Schaible, E. Gann, R. Kirian, A. MacDowell, M. Church, B. Rude and H. Padmore, *J. Phys. Conf. Ser.*, 2010, **247**, 012007.

2 J. Jing, S. Dong, K. Zhang, Z. Zhou, Q. Xue, Y. Song, Z. Du, M. Ren and F. Huang, *Adv. Energy Mater.*, 2022, **12,** 2200453.

3 X. Huang, L. Zhang, Y. Cheng, J. Oh, C. Li, B. Huang, L. Zhao, J. Deng, Y. Zhang, Z. Liu, F. Wu, X. Hu, C. Yang, L. Chen and Y. Chen, *Adv. Funct. Mater*., 2022, **32**, 2108634.

4 C. Xu, K. Jin, Z. Xiao, Z. Zhao, X. Ma, X. Wang, J. Li, W. Xu, S. Zhang, L. Ding and F. Zhang, *Adv. Funct. Mater*., 2021, **31**, 2107934.

5 Y. Xie, Y. Cai, L. Zhu, R. Xia, L, Ye, X. Feng, H.-L. Yip, F. Liu, G. Lu, S. Lu, S. Tan and Y. Sun, *Adv. Funct. Mater*., 2020, **30**, 2002181.

6 T. Xu, Y. Luo, S. Wu, B. Deng, S. Chen, Y. Zhong, S. Wang, G. Lévêque, R. Bachelot and F. Zhu, *Adv. Sci*., 2022, **9**, 2202150.

7 W. Wang, C. Yan, T. Lau, J. Wang, K. Liu, Y. Fan, X. Lu and X. Zhan, *Adv. Mater*. 2017, **29**, 1701308.

8 T. Li, S. Dai, Z. Ke, L. Yang, J. Wang, C. Yan, W. M and X. Zhan, *Adv. Mater*., 2018, **30**, 1705969.

9 C. Chang, L. Zuo, H. Yip, Y. Li, C. Li, C.-S. Hsu, Y. Cheng, H. Chen and A. K. Jen, *Adv. Funct. Mater*., 2013, **23**, 5084–5090.

10 C. Chen, L. Dou, J. Gao, W. Chang, G. Li and Y. Yang, *Energy Environ. Sci*., 2013, **6**, 2714.

11 X. Huang, J. Oh, Y. Cheng, B. Huang, S. Ding, Q. He, F. Wu, C. Yang, L. Chen and Y. Chen, *J. Mater. Chem. A*, 2021, **9**, 5711.

12 Y. L, J. Lin, X. Che, Y. Qu, F. Liu, L. Liao and S. R. Forrest, *J. Am. Chem. Soc*., 2017, **139**, 17114-17119.

13 B. Jia, S. Dai, Z. Ke, C. Yan, W. Ma and X. Zhan, *Chem. Mater*., 2018, **30**, 239−245.

14 Y. Cui, C. Yang, H. Yao, J. Zhu, Y. Wang, G. Jia, F. Gao and J. Hou, *Adv. Mater*., 2017, **29**, 1703080.

15 F. Liu, Z. Zhou, C. Zhang, J. Zhang, Q. Hu, T. Vergote, F. Liu, T. P. Russell and X. Zhu, *Adv. Mater*., 2017, **29**, 1606574.

16 M. Luo, C. Zhao, J. Yuan, J. Hai, F. Cai, Y. Hu, H. Peng, Y. Bai, Z. Tan and Y. Zou, *Mater. Chem. Front*., 2019, **3**, 2483-2490.

17 Y. Xie, L. Huo, B. Fan, H. Fu, Y. Cai, L. Zhang, Z. Li, Y. Wang, W. Ma, Y. Chen and Y. Sun, *Adv. Funct. Mater*. 2018, **28**, 1800627.

18 P, Cheng, H. Wang, Y. Zhu, R. Zheng, T. Li, C. Chen, T. Huang, Y. Zhao, R. Wang, D. Meng, Y. Li, C. Zhu, K. Wei, X. Zhan and Y. Yang, *Adv. Mater*., 2020, **32**, 2003891.

19 H. Wang, P. Cheng, S. Tan, C. Chen, B. Chang, C. Tsao, L. Chen, C. -A. Hsieh, Y. Lin, H. Cheng, Y. Yang and K. Wei, *Adv. Energy Mater*., 2021, **11**, 2003576.

20 H. I. Jeong, S. Biswas, S. C. Yoon, S. Ko, H. Kim and H. Choi, *Adv. Energy Mater*., 2021, 2102397.